Application of Mamdani Fuzzy Inference Systems to Interference Assessments

Samuel Hussey
Department of Electrical and
Computer Engineering
Baylor University
Waco, TX
Samuel_Hussey1@baylor.edu

Jonathan E. Swindell
Department of Electrical and
Computer Engineering
Baylor University
Waco, TX
Jonathan Swindell1@baylor.edu

Adam C. Goad
Department of Electrical and
Computer Engineering
Baylor University
Waco, TX
Adam Goad@baylor.edu

Austin Egbert

Department of Electrical and

Computer Engineering

Baylor University

Waco, TX

Austin Egbert@baylor.edu

Andrew Clegg
Department of Electrical and
Computer Engineering
Baylor University
Waco, TX
Andy_Clegg@baylor.edu

Charles Baylis
Department of Electrical and
Computer Engineering
Baylor University
Waco, TX
Charles_Baylis@baylor.edu

Robert J. Marks II

Department of Electrical and

Computer Engineering

Baylor University

Waco, TX

Robert Marks@baylor.edu

Abstract—In dynamic spectrum allocation involving passive wireless systems, such as for weather radiometry or radio astronomy, estimating potential interference is crucial in setting transmission spectral and spatial limitations for potentially interfering transmitters. The challenge in accurately assessing interference is heightened by variability in environmental factors and limitations of static modeling. This often leads to protection levels that are either excessively stringent or overly permissive. Dynamic spectrum access (DSA) systems commonly rely on the ability to precisely model transmissions and estimate interference prior to frequency assignment, where total interfering power is acquired by means of summing individual contributions to a potential victim receiver. As an alternative to the worst-case static calculations, this paper proposes the implementation of a Mamdanitype fuzzy inference system as the assessment mechanism for interference levels. In this approach, transmitter operations and network characteristics are characterized by their degree of membership with various linguistic variables. Membership grades are then provided to a ruleset determined by the expected relationship between input and output parameters. The value implied by the rules gives an estimation of interfering power level that may be tuned by adjusting the membership characterization of parameters. After tuning, simulation results yield a Root Mean Square Error (RMSE) improvement of approximately 39%, demonstrating the system's ability to adapt to varying levels of agreement with static calculations.

Keywords—interference, spectrum management, fuzzy inference systems, dynamic spectrum access

I. INTRODUCTION

The advent of fifth-generation (5G) mobile broadband has introduced a number of improvements over previous generations including higher data rates, reduced latency, and improved coverage in rural areas. The tradeoffs necessary to achieve these improvements have proved cumbersome for other wireless services, especially critical passive services such as weather

radiometry and radio astronomy. High bandwidth needs have resulted in the allocation of large blocks of spectrum to 5G in recent years, in addition to many allocations interleaved among previously established services. While the 5G standard and spectrum policy implement emission limits, concerns regarding their efficacy in scenarios involving passive systems remains due to disagreement between compatibility studies conducted to inform policy makers [1]. For example, the auction of 24 GHz spectrum to 5G wireless services has created such a scenario and presents a notable risk to passive radiometers operating in the 23.6 – 24.0 GHz Earth Exploration-Satellite Service (EESS) band [2].

It can be difficult for DSA systems to acquire the information needed to predict compatibility with sufficiently low error and choose an appropriate propagation model given inherent uncertainties [3]. This makes calculations to classify interference difficult to execute with high precision and reasonableness for complex propagation environments. At millimeter wavelengths, minor errors in location and antenna positioning data coupled with phenomena such as multipath effects can make deterministic interference calculations intractable. The issue of complexity is further exacerbated when considering the aggregation of interferences from simultaneous transmissions.

In response to the difficulties of precisely modeling networks and their propagation environments, many works have developed statistical models aiming to reduce the computational complexity of interference predictions by assigning probability distributions to parameters with random variations [4]-[7]. Peng et al. describe another simplified method of aggregating interference to deepspace Earth stations from high-density fixed service (HDFS) emitters in which the area surrounding deep-space Earth stations is geometrically partitioned and used to model the correlation of interferences [8]. Authors in [9]-[11] consider models that estimate total interference in scenarios where emitters are distributed uniformly over a region surrounding a primary receiver.

Other methods for interference prediction that have been explored recently have leveraged machine learning (ML) algorithms to handle analytically intractable calculations. Padilla presents a nonlinear autoregressive neural network (NARNN) to predict interference and aid in efficient resource allocation [12]. Saija evaluates the ability of various ML algorithms to estimate channel state information (CSI) in 5G systems by predicting signal-to-noise ratio (SNR) and shows that the ML approaches outperform traditional methods in terms of error [13]. Zhao demonstrates a method wherein location, path loss information, and transmit power are supplied from a network of transmitters to a backpropagation neural network trained to predict aggregate interference at a receiver [14].

These prior works have produced important results by successfully reducing the complexity of interference analysis, but many existing techniques remain unsuitable for real-time spectrum management applications. For example, the Citizens Broadband Radio Service (CBRS) Spectrum Access System (SAS) aggregate interference assessments encompass millions of path loss calculations, often delaying spectrum assignment for 24 or more hours [15]. ML-based approaches provide adequate speed but lack an explanation facility able to offer insights regarding the decisions of the assessment mechanism, a feature that may be desirable when mischaracterizations occur. In the event inconsistent results are produced by ML-based approaches actions are generally limited to error analysis, data inspection, and further training of the network to address the unknown contingencies introducing error.

Fuzzy inference systems (FIS) lend themselves well to interference prediction due to their tolerance for uncertainties in provided data, tunable nature, and inherent explanation facility. Incorporated with a DSA controller such as a spectral broker [16], an FIS accepts precise and ambiguous information alike and can perform the evaluation within the time and computational constraints of the brokering system. A spectral broker can be used to coordinate between active and passive spectrum users, and can provide limitations for transmission by active users to avoid interference with passive services [17]. This paper introduces the design of a Mamdani-type FIS tuned to a coexistence scenario between 5G devices and passive radiometers whose frequency assignments are managed by a spectral brokering system.

II. BACKGROUND

A. Fuzzy Inference Primer

In conventional crisp logic, an element's membership in a set is binary. As an alternative, L. A. Zadeh proposed Fuzzy Sets in 1964 [18]. Fuzzy Sets describe the degree to which an element belongs to a set. As with crisp logic, union and intersection operations are defined that facilitate the comparison of sets. By applying fuzzy logic to control systems, fuzzy inference systems can accurately model system behavior and have been validated by their reduction to practice. In a study on the impact of Fuzzy Logic conducted in 2013, there were 26 journals, over 100,000 publications, and over 2500 patents in the United States and Japan [19].

FISs provide a mathematical framework for human decision making consisting of three primary stages: fuzzification, rule evaluation, and defuzzification. For purposes of clarity, a tutorial example of fuzzy inference is provided. The example considers two leading indicators of graduate student performance: grade-point average (GPA) and Graduate Record Examinations (GRE) scores. In this example, each antecedent has three membership functions: μ_P , μ_F , and μ_H , where P is poor, F is fair, and H is high. Plots of these membership functions are shown in Figs. 1 and 2.

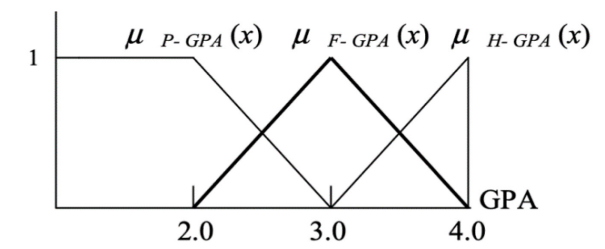


Fig. 1. GPA antecedent membership functions

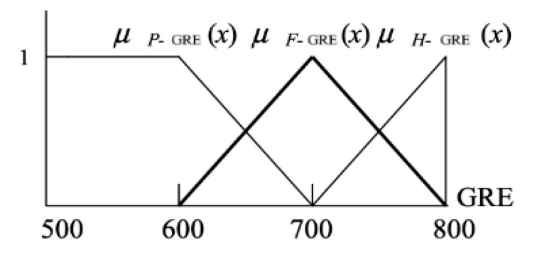


Fig. 2. GRE antecedent membership functions

During the fuzzification process, each membership function illustrated in the figures above is evaluated for the corresponding input, resulting in the degree to which an input belongs to that fuzzy set. Consider a student with a GPA of 3.5 and a GRE score of 775. This GPA has no membership with the set of poor scores and belongs equally to the fair and high sets; $\mu_P = 0, \mu_F = 0.5, \mu_H = 0.5$. The GRE score also has no membership with the set of poor scores and belongs predominately to the high set compared to the fair set; $\mu_P = 0, \mu_F = 0.25, \mu_H = 0.75$. These resulting membership grades are used in the rule evaluation stage.

Rule evaluation maps the membership grades of each input to a scaling factor for each consequent membership function. In general, two primary approaches are used to construct a rule table. First, a subject matter expert can use their expertise to codify rules about the behavior of the system. Second, an optimization method can be applied to find a set of rules that minimize a cost function describing the difference between the system output and target value. When the rule table can be constructed based on expertise, this provides intuition regarding how the system arrived at an output. This is a significant benefit of Fuzzy Inference Systems compared to other artificial intelligence methods.

To model the relationship between students' scores and anticipated performance, a domain expert such as an experienced professor constructs the rule set in Table I. The rows and columns correspond to the fuzzy sets for poor, fair, and high scores while the cells at their intersections correspond to the implied fuzzy sets for poor, average, good, and excellent student performances. Poor GRE and poor GPA implies poor graduate student, fair GRE and fair GPA implies average graduate student, and so on for all cases. The membership grades for GPA and GRE scores of 3.5 and 775 are given next to their respective sets. Cells are assigned their values by taking the minimum value of their respective row and column.

TABLE I. GRADUATE STUDENT TYPE IMPLIED BY GPA AND GRE

Grad Student		GPA		
Туре		P → 0	F → ½	H → ½
G	P → 0	P → 0	P → 0	P → 0
R	F → ½	P → 0	A→¹/₄	G → ¼
Е	H → ¾	P → 0	G → ½	E → ½

In this example, the final output will be a graduate student ranking between 0 and 10, where greater values correspond to a better graduate student. To map between the rule table and output, four consequent membership functions are used: μ_P , μ_A , μ_G , and μ_E , where P is poor, A is average, G is good, and E is excellent. Plots of these functions can be seen in Fig. 3.

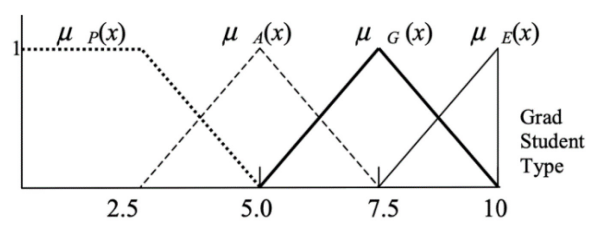


Fig. 3. Consequent membership functions

Cell values from the rule table are used to scale the consequent fuzzy sets' membership functions. In the case that there are multiple cells for the same fuzzy set, the maximum value of the group is taken to be the final weight. Thus, from Table I, $\mu_P=0$, $\mu_A=0.25$, $\mu_G=0.5$, and $\mu_E=0.5$. The scaled consequent membership functions are shown in Fig. 4.

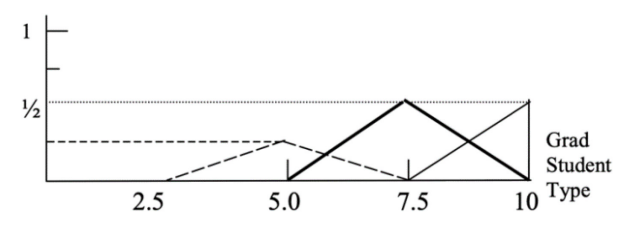


Fig. 4. Consequent membership functions scaled by rule table weights

In the defuzzification stage, the scaled membership functions are summed as shown in Fig. 5. A number of defuzzification methods exist and have application-specific trade-offs. The center of mass method is commonly used. The center of mass of the weighted membership functions, in general, is given by:

$$d = \frac{\int_{-\infty}^{\infty} \sum_{n} a_{n} x \mu_{n}(x) dx}{\int_{-\infty}^{\infty} \sum_{n} a_{n} \mu_{n}(x) dx}$$
(1)

where the summation is over all of the consequent membership functions, $\{\mu_n(x)\}$, and their corresponding weights, $\{a_n\}$. If the area under the n^{th} membership function is given by:

$$A_n = \int_{-\infty}^{\infty} \mu_n(x) dx \tag{2}$$

and center of mass:

$$c_n = \frac{\int_{-\infty}^{\infty} x \mu_n(x) dx}{A_n} \tag{3}$$

Then the defuzzification can be written as:

$$d = \frac{\sum_{n} a_n c_n A_n}{\sum_{n} a_n A_n} \tag{4}$$

Applying this defuzzification method to the example returns the final crisp output d = 7.3.

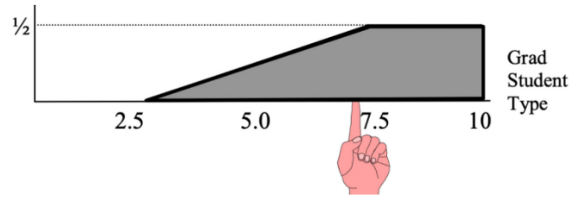


Fig. 5. The center of mass of the sum of the weighted membership functions

B. Spectral Brokering

Similar in principle to the automated frequency coordination (AFC) system at 6 GHz and SAS in the 3.5 GHz band, the cooperative brokering system coordinates spectrum use between active and passive users by considering spectral, spatial, and temporal resource use in its network and implementing constraints on potentially interfering devices [17]. To determine potential interferers, the spectral resources desired by a user are submitted as a request to the broker. With this information the broker begins assessing the most recently submitted request against existing allowances of other devices, covering all combinations of device pairs.

In each assessment, five stages of culling take place in which the broker evaluates overlap between parameters. The first three stages look for time overlap of the requests, whether the devices are within line of sight of each other, and whether the main beam of the transmitter's antenna pattern intersects the location of the other device. In stage four, free space path loss (FSPL) calculations determine whether power of a transmission will exceed the interference tolerance of the receiving device. The final stage performs frequency interference calculations by first looking for direct overlap between requested bands, then for out-of-band interference potential.

Each stage of analysis can short-circuit subsequent stages, meaning that, if at any point in the culling process no overlap is determined, then each device in the pair of devices under evaluation will be considered to be free of potential interference from the other, and the broker will proceed to the next pair immediately, bypassing the remaining stages. If none of the five stages of the culling process rule out the potential for interference, the broker will generate a spatial-spectral mask for the interferer that limits transmission power as a function of frequency and direction. If no interference is expected from any individual device, the broker then, making worst-case assumptions, sums the powers of transmissions at each receiver's location to estimate the total levels of interference that may be seen. If the aggregated

signal level exceeds the device's interference tolerance, a spatial-spectral mask is provided to the most recent user to submit a request for spectrum.

An alternative to the current worst-case method utilized by the broker, which considers no fading and assumes fully constructive interference, should be evaluated. The nature of the inference process and its tuning to a specific coexistence environment address uncertainties in propagation and equip the broker with the flexibility needed to extend to other spectrum sharing scenarios.

III. NETWORK MODEL

A. Network Topology

To simulate the environment for evaluating interference, we consider a homogeneous network comprised of a single radiometer among a set of 5G transmitters. The transmitters are spaced approximately the same distances from one another, while the radiometer location varies across the approximately 1 km² region encompassing the devices. Fig. 6 shows an example of the network containing three 5G transmitters with a single radiometer placed at the center of the coexistence space.

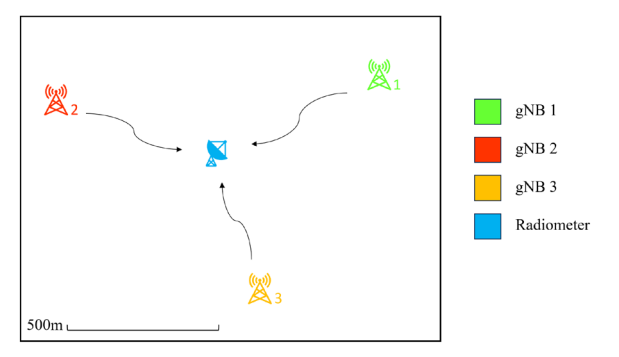


Fig. 6. Device placement in network area of approximately 1 km²

B. Modeling Devices

Spectrum consumption models (SCMs) are used to represent devices in our simulations. SCMs are a data structure made up of 11 data elements, each articulating some aspect of spectrum use [20]. Transmitter models capture the RF emissions of a transmitting device by identifying location of the device, operating times, a spectral mask (how much power is transmitted at frequencies of interest), and directivity. Receiver models define interference thresholds for a receiving device by capturing its location, operating times, an underlay mask (power tolerance values at frequencies of interest), directivity of reception, and susceptance to intermodulation effects.

The power level for each transmitter is captured as effective isotropic radiated power (EIRP) in the direction of the radiometer and within its 200 MHz channel. The radiometer tolerance is captured as a power spectral density (PSD) with a center operating frequency of 23.84 GHz. The PSD of out-of-band emissions into the passive EESS band was modeled to range from -70 to -40 dBW/200 MHz, well below the recommended limit published in [21], but high enough to interfere in aggregate depending on the relative locations of devices.

C. Data Generation

The simulated network is used to generate a synthetic dataset made up of transmitted PSDs and distances between devices as inputs and the interfering PSDs after path loss as outputs. To acquire different propagation distances, the location of the radiometer is swept across the network's geographical area. At each location, the interfering power is calculated across the range of out-of-band emission powers given FSPL between devices. FSPL is justified here by the relatively short distances over which the 5G/radiometer coexistence is analyzed. The final dataset captured for use by the FIS consists of a range of PSDs in the observation channel of the radiometer, distances between transmitters and radiometer, and the individual interfering powers at each location.

In total, the full dataset consists of approximately 71000 points. Because FIS tuning is similar in nature to training an ML-model it is necessary to apportion the data into training and validation subsets to ensure good generalization. These subsets comprise 80% and 20% of the total dataset respectively.

IV. MAMDANI FUZZY INFERENCE SYSTEM DESIGN

With knowledge of device location, orientation, and antenna characteristics, the spectral broker is able to provide, as inputs to the FIS, the distance between devices under assessment and the transmitter PSD in the direction of interest. The variables chosen to describe the inputs and outputs of this design are simply "low", "medium", and "high". The rule base is formed by our chosen linguistic variables and the known relationship between distance and pathloss. Results of the rule evaluation are then used as weights for the consequent membership functions. The final defuzzied value is acquired from the centroid of the weighted and summed consequent membership functions as previously described in the fuzzy inference primer.

A. Antecedent Membership Functions

Our design considers only transmitted PSD and distance between devices. Functions of low, medium, and high transmit PSDs and distances are initially crafted based on the range of values available in the synthetic dataset. For the PSDs of emissions, input values are bounded between -70 and -40 dBW/200 MHz. Shown in Fig. 7, low membership increases as the input value approaches the lower bound, high membership peaks at the opposite end of the plot, and medium membership is maximized in the middle of the input range while overlapping surrounding functions. Functions for distance, shown in Fig. 8, are crafted in a similar manner with values ranging from approximately 50 to 1650 meters.

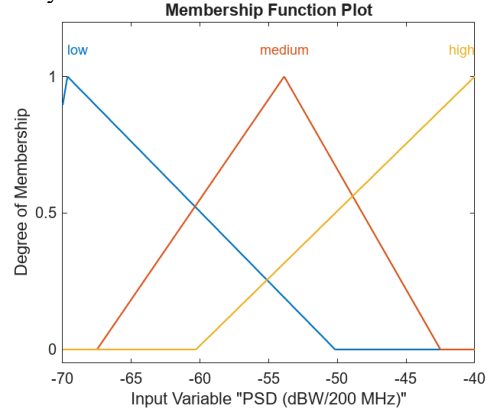


Fig. 7. Transmitter PSD (dBW/200 MHz) membership functions

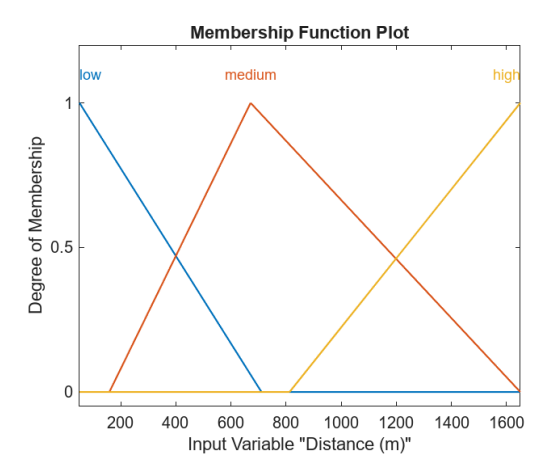


Fig. 8. Distance (m) membership functions

B. Rule Evaluation

The implications that drive fuzzy inference are captured by a set of rules describing the relationship between antecedents and consequents. Rules are crafted based on expert intuition and domain knowledge. Though trivial in this case, the implications of more complicated systems require additional knowledge and may be captured by a larger rule base. The set of rules used in this design is shown in Table II.

TABLE II. FUZZY INFERENCE SYSTEM RULE TABLE

	Rule
1	If (PSD is Low) and (Distance is Low) then (Interfering PSD is Medium)
2	If (PSD is Medium) and (Distance is Low) then (Interfering PSD is High)
3	If (PSD is High) and (Distance is Low) then (Interfering PSD is High)
4	If (PSD is Low) and (Distance is Medium) then (Interfering PSD is Low)
5	If (PSD is Medium) and (Distance is Medium) then (Interfering PSD is Medium)
6	If (PSD is High) and (Distance is Medium) then (Interfering PSD is High)
7	If (PSD is Low) and (Distance is High) then (Interfering PSD is Low)
8	If (PSD is Medium) and (Distance is High) then (Interfering PSD is Low)
9	If (PSD is High) and (Distance is High) then (Interfering PSD is Medium)

C. Consequent Membership Functions

FSPL indicates approximately 94 to 124 dB of loss over 50 – 1650 meters, the smallest and largest distances separating devices in the simulated network respectively. From these values and the range of input PSDs, a reasonable range of output values was determined to be -195 to -150 dBW/200 MHz, where -166 dBW/200 MHz or greater is assumed to inflict harmful interference [22]. Similar to the antecedents, the consequent membership functions shown in Fig. 9 are triangular with functions for low and high peaking at opposite ends of the plot and the function of medium PSDs encompassing values in between with some overlap.

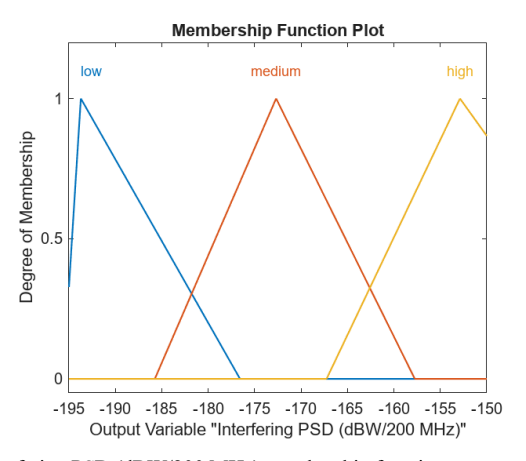


Fig. 9. Interfering PSD (dBW/200 MHz) membership functions

V. SIMULATION RESULTS

The FIS can function immediately upon implementation but benefits from a training period in which the membership functions and rule base are optimized to infer results more accurately. Membership function tuning was performed in MATLAB using the Global Optimization Toolbox, Fuzzy Logic Toolbox, and the Parallel Computing Toolbox. After tuning, the inference process may be reduced to a simple look-up table operation. A visualization of the control surface generated from this table is shown in Fig. 10. The trends illuminated by this graphic agree with those described by FSPL. As the distance between devices decreases or the transmission PSD increases, the potential interference increases.

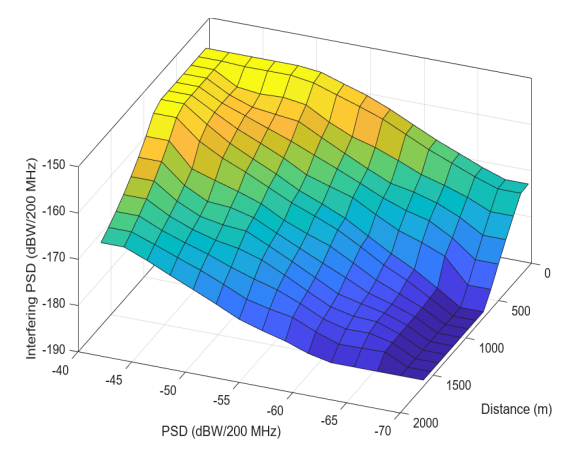


Fig. 10. FIS control surface

To assess performance, the FIS was evaluated on the validation dataset. Prior to any optimization, an RMSE of 2.623 dB was attained. After tuning, this value was reduced to 1.598 dB, corresponding to a Mean Absolute Percent Error (MAPE) of 0.686%. Note that because the FIS holds no notion of the scale on which the data resides, the MAPE and RMSE were calculated based on the numerical value of the outputs. Fig. 11 illustrates the results succinctly. The solid y = x line describes a perfect interference level prediction. Our model's predictions and the target values fall on the x and y axes respectively, the blue circles indicating the intercept point. The distance between each circle and the solid line represents the error as a dB difference. Though there appears to be a significant amount of variance, 95% of points fall within the dashed lines representing 2σ , where $\sigma = 1.077$ dB.

These results demonstrate that this preliminary implementation can reach an adequate level of agreement with a well understood propagation model. Should it be decided that the interference estimations given by that model are too permissive for a given application, additional data and tuning of the FIS can provide more acceptable results.

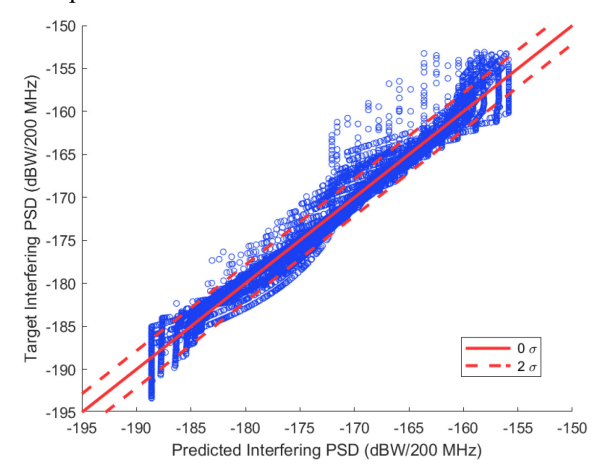


Fig. 11. Predicted Interference Levels After Tuning

VI. CONCLUSION

An FIS design has been presented which can predict interference while reducing complexity of calculations. In this approach, the ambiguity inherent in modeling propagation environments and spectrum usage is handled by the fuzzy mathematical framework and can be used to enable departure from worst-case assumptions in interference assessments by tuning individual contributions to more or less stringent approximations depending upon application. Simulation results show that, after tuning, the system reaches reasonable agreement with FSPL estimations. This implies that the FIS, given additional input parameters, membership functions, and rules, may be tuned to match more complicated propagation models and interference scenarios that previously relied heavily on statistical models or other black-box style approaches.

ACKNOWLEDGMENT

This work has been funded by the National Science Foundation (Grant No. 2030243).

REFERENCES

- Summary of Studies Performed in TG 5/1 For Protection of Passive EESS in Band 23.6-24 GHz, ITU Doc CPM19-2/99-E (6 February 2019).
- [2] D. Lubar, D. Kunkee, and L. Cahsin, "Developing a Sustainable Spectrum Approach to Deliver 5G Services and Critical Weather Forecasts," in Center for Space Policy and Strategy, The Aerospace Corporation, January 2020.
- [3] J. Riihijarvi, D. Maibam, and P. Mahonen, "Impact of model uncertainties on quantitative evaluation of interference risks," 2017 IEEE International Symposium on Dynamic Spectrum Access Networks (DySPAN), Mar. 2017. doi:10.1109/dyspan.2017.7920776
- [4] "Characterization and assessment of aggregate interference to Earth exploration-satellite service (passive) sensor operations from mulitple sources of man-made emissions", Recommendation ITU-R RS.1858 (01/2010)
- [5] A. Ghasemi and E. S. Sousa, "Interference Aggregation in Spectrum-Sensing Cognitive Wireless Networks," in IEEE Journal of Selected Topics

- in Signal Processing, vol. 2, no. 1, pp. 41-56, Feb. 2008, doi: 10.1109/JSTSP.2007.914897.
- [6] S. Kusaladharma and C. Tellambura, "Aggregate Interference Analysis for Underlay Cognitive Radio Networks," in IEEE Wireless Communications Letters, vol. 1, no. 6, pp. 641-644, December 2012, doi: 10.1109/WCL.2012.091312.120600.
- [7] L. Vijayandran, P. Dharmawansa, T. Ekman and C. Tellambura, "Analysis of Aggregate Interference and Primary System Performance in Finite Area Cognitive Radio Networks," in IEEE Transactions on Communications, vol. 60, no. 7, pp. 1811-1822, July 2012, doi: 10.1109/TCOMM.2012.051412.100739.
- [8] Peng, T., Kinman, P., Kayalar, S., and Ho, C., "Estimating the Aggregate Interference from High-Density Fixed Service Emitters to Deep-Space Earth Stations", Interplanetary Network Progress Report, vol. 42–179, pp. 1–27, 2009.
- [9] S. Bhattarai, A. Ullah, J. -M. J. Park, J. H. Reed, D. Gurney and B. Gao, "Defining incumbent protection zones on the fly: Dynamic boundaries for spectrum sharing," 2015 IEEE International Symposium on Dynamic Spectrum Access Networks (DySPAN), Stockholm, Sweden, 2015, pp. 251-262, doi: 10.1109/DySPAN.2015.7343908.
- [10] S. Bhattarai, J.-M. Jerry Park, W. Lehr and B. Gao, "TESSO: An analytical tool for characterizing aggregate interference and enabling spatial spectrum sharing," 2017 IEEE International Symposium on Dynamic Spectrum Access Networks (DySPAN), Baltimore, MD, USA, 2017, pp. 1-10, doi: 10.1109/DySPAN.2017.7920793.
- [11] N. H. Mahmood, F. Yilmaz, M.-S. Alouini, and G. E. Oien, "Cognitive interference modeling with applications in power and admission control," 2012 IEEE International Symposium on Dynamic Spectrum Access Networks, Oct. 2012. doi:10.1109/dyspan.2012.6478167
- [12] C. Padilla, R. Hashemi, N. H. Mahmood and M. Latva-Aho, "A Nonlinear Autoregressive Neural Network for Interference Prediction and Resource Allocation in URLLC Scenarios," 2021 International Conference on Information and Communication Technology Convergence (ICTC), Jeju Island, Korea, Republic of, 2021, pp. 184-189, doi: 10.1109/ICTC52510.2021.9620845.
- [13] K. Saija, S. Nethi, S. Chaudhuri and R. M. Karthik, "A Machine Learning Approach for SNR Prediction in 5G Systems," 2019 IEEE International Conference on Advanced Networks and Telecommunications Systems (ANTS), Goa, India, 2019, pp. 1-6, doi: 10.1109/ANTS47819.2019.9118097.
- [14] Y. Zhao, L. Shi, X. Guo and C. Sun, "Aggregate Interference Prediction Based on Back-Propagation Neural Network," 2018 IEEE International Symposium on Dynamic Spectrum Access Networks (DySPAN), Seoul, Korea (South), 2018, pp. 1-5, doi: 10.1109/DySPAN.2018.8610415.
- [15] FCC Technical Advisory Council, "Recommnedations to the Federal Communications Commission Based on Lessons Learned from CBRS,"

 December, 2022. [Online]. Available: https://www.fcc.gov/sites/default/files/recommendations_to_the_federal_c ommunications commission based on lessons learned from cbrs.pdf
- [16] J. Marino and A. J. Gasiewski, "A Broker Based Scheme for Spectrum Sharing," 2017 IEEE International Geoscience and Remote Sensing Symposium (IGARSS), 2017, pp. 3455-3458, doi: 10.1109/IGARSS.2017.8127742.
- [17] S.A. Seguin, A. Goad, C. Baylis, R.J. Marks, "Spectrum Sharing Brokers for Active and Passive Devices," 2022 IEEE International Symposium on Electromagnetic Compatibility and Signal/Power Integrity, Spokane, Washington, August 2022.
- [18] L. A. Zadeh, "Fuzzy sets," Information and Control, vol. 8, no. 3, pp. 338–353, Jun. 1965, doi: 10.1016/S0019-9958(65)90241-X.
- [19] H. Singh et al., "Real-Life Applications of Fuzzy Logic," Advances in Fuzzy Systems, vol. 2013, p. e581879, Jun. 2013, doi: 10.1155/2013/581879.
- [20] IEEE, "IEEE 1900.5.2-2017 IEEE standard for method for modeling spectrum consumption," 2017.
- [21] "Compatibility between Earth exploration-satellite service (passive) and relevant active services", Resolution 750 (REV.WRC-19) (2020).
- [22] "Performance and interference criteria for satellite passive remote sensing", Recommendation ITU-R RS.2017-0 (08/2012)